Research Square

Preprints are preliminary reports that have not undergone peer review.
They should not be considered conclusive, used to inform clinical practice,
or referenced by the media as validated information.

Pulsatility Protects the Endothelial Function during Extracorporeal Membrane Oxygenation

Yu Zhang
Guangdong Provincial Hospital of Traditional Chinese Medicine
Jianfeng Zeng
Sun Yat-Sen Memorial Hospital
Jiani Li
Guangdong Provincial People's Hospital
Xiaoqian He
Guangzhou Women and Children's Medical Center
Guanhua Li (dr.liguanhua@hotmail.com)
Sun Yat-Sen Memorial Hospital

Research

Keywords: pulsatility, extracorporeal membrane oxygenation, peak wall shear stress, endothelial glycocalyx, microcirculation

Posted Date: January 29th, 2021

DOI: https://doi.org/10.21203/rs.3.rs-157787/v1

License: This work is licensed under a Creative Commons Attribution 4.0 International License.
Read Full License

Abstract

Background

Pulsatile flow has been proved to protect vital organ function and microcirculation during extracorporeal membrane oxygenation (ECMO). Studies revealed that pulsatile shear stress plays a vital role in the microcirculatory function and integrity. The objective of this study was to investigate how pulsatility affects wall shear stress and microcirculation during ECMO.

Methods

Using the i-Cor system, we compared the effects of pulstile or non-pulsatile flows in a canine ECMO model, with hemodynamic parameters and peak wall shear stress (PWSS) calculated. Serum concentrations of syndecan-1 and heparan sulfate were measured at different time points during ECMO. Pulstile shear stress experiments were also validated in endothelial cells exposed to different magnitude of pulsatility, with cell viability, the expressions of syndecan-1 and endothelial-to-mesenchymal tranformation (EndMT) markers analyzed.

Results

The pulsatile flow generated more surplus hemodynamic energy and preserved higher PWSS during ECMO. Serum concentrations of syndecan-1 and heparan sulfate were both negatively correlated with PWSS, and significantly lower levels were observed in the pulsatile group. In addition, non-pulsatility triggered EndMT, with EndMT related genes up-regulated, and endothelial cells exposed to low pulsatility had the lowest possibility of EndMT.

Conclusion

The maintenance of the PWSS by pulsatility during ECMO contributes to the beneficial effects on glycocalyx integrity and microcirculatory function. Moreover, pulsatility prevents EndMT in endothelial cells, and low pulsatility exhibits the best protective effects. The augmentation of pulsatility may be a future direction to improve the clinical outcome in ECMO.

Introduction

Extracorporeal membrane oxygenation (ECMO), a life-saving approach, is essentially important for the treatment of patients with severe cardiorespiratory failure, including those extremely critical COVID-19 patients[1], however, overall survival rate for extracorporeal life support (ECLS) is increasing sluggishly over the past ten years[2]. While ECLS rescues the cardiorespiratory sytem, microcirculatory malperfusion easily occurrs when prolonged ECLS is executed as the continuous non-physiological flow impairs the

microcirculatory function[3]. Microcirculatory disturbance has been identified as an independent risk factor for mortality during ECMO[4]. It is generally acknowledged that microcirculatory malperfusion affects the endothelial integrity, which leads to hypoxia, edema, acidosis, and inflammatory responses.

Currently, the standard circuit consists of a membrane oxygenator and centrifugal pump, of which the priming volume is smaller, with lower incidence of blood component damage[5]. However, one of its main drawbacks is the typically non-pulsatile flow, of which the non-physiological nature leads to malperfusion to peripheral tissue and microcirculation[6]. Recently, several pumps that can produce pulsatile flow for ECLS circuits have been developed[3, 7, 8]. The novel i-Cor system (Xenios AG, Heilbronn, Germany) consists of a diagonal blood pump that can provide pulsatile flow triggered by electrocardiogram and has been applied in Europe for several years[9, 10]. Ündar`s group used the i-Cor system in animal models with both flow patterns and had reported that the renal function and vascular hemodynamics were better in the pulsatile group as compared to the non-pulsatile group[7].

The advantages of pulsatile flow have been well-established in the mechanical circulatory support system, including conventional cardiopulmonary bypass, ECMO, and ventricular assist devices. Pulsatile flow generates more optimal hemodynamic energy and extra-pressure[11], which preserved microcirculatory perfusion[12], and subsequently alleviates systemic inflammatory responses[13]. Endothelial dysfunction has been proved to be a crucial determinant of microcirculatory disturbance. The microvascular endothelial cell facilitates the microcirculatory exchanges of biological molecules, participating in various pathophysiological processes like inflammation, angiogenesis, vascular permeability, and so on[14].

The glycocalyx, formed by proteoglycans, glycosaminoglycan chains, and membrane glycoproteins, coats the inner surface of endothelium and provides protective layers, directly affecting the microcirculatory intergrity and function[15]. Extensive research has proved that glycocalyx is also a mechanosensor[16], and a stable wall shear stress balances between biological synthesis and degradation in glycocalyx[17, 18]. Assmann et al. [19] revealed that non-pulsatile flow in cardiopulmonary bypass decreases peak wall shear stress (PWSS) and causes elevations of syndecan-1 and heparan sulfate, both of which are the by-products for glycocalyx degradation. However, the correlation between shear stress and microcirculation during ECMO is poorly understood. In this study, we investigated the relationship between shear stress and microcirculatory function, which was detected by glycocalyx degradation by-products, in an attemp to determine whether pulsatile flow under ECMO improves microcirculation and preserves endothelial function.

Materials And Methods

Ethical approval was obtained from the Institutional Animal Care and Use Committee of Sun Yat-sen Memorial Hospital (Reference No. SYSU-IACUC-2020-B0402). The experimental setting was established in accordance with the Guide for the Care and Use of Laboratory Animals by the National Institute of Health (NIH) of the United States (revised in 1985).

Study design

To evaluate the pulsatile flow as a mediator of shear stress under ECMO, both in vitro and in vivo models were developed. For the in vivo model, we developed a canine model with cardiogenic shock, which was supported by pulsatile or non-pulsatile mode of ECLS established by the i-Cor system. Pulsatile flow and continuous flow were compared in canine models with respect to hemodynamics, shear stress, and endothelial integrity. The correlation between shear stress and syndecan-1 level was also studied. For the in vitro model, the Flexcell system (Flexcell Inc., McKee-sport, PA, USA), a biofluid mechanics device was employed. Pulmonary microvascular endothelial cells (PMVECs) were cultured under the Flexcell system with continuous flow or pulsatile flow with different shear stresses. After a dynamic cultivation, the effect of flow patterns on PMVEC viability, expression of syndecan-1, and possiblity of endothelial to mesenchymal transformation (EndMT) were investigated.

ECMO settings

The experimental ECMO settings consisted of a console (i-Cor, Xenios AG, Heilbronn, Germany), a diagonal pump that can easily generated pulsatility, a gas blender (Sechrist, Whitewright, TX, USA) and a membrane oxygenator (Medos Medizintechnik AG, Stolberg, Germany). To prime the ECLS circuit, 200 mL Ringer`s solution was employed, with a pump rate set at 70 beats per minute (bpm) during ECMO. PaO_2 ranging from 10 kPa to 16 kPa, and $PaCO_2$ from 4.0 kPa to 6 kPa were maintained for the oxygen / airflow, as suggested by previous publications[10]. Switching from continuous flow to pulsatility could be easily achieved via the i-Cor system. Triggered and synchronized by electrocardiogram (ECG), the pulsatile flow runs in an equivalent fashion (1:1) if the heart rate (HR) was lower than 100bpm. Intravenous verapamil (1.5mg) was administered in case of tachycardia (HR > 120 bpm) to maintain a pulsatility at a parallel ratio.

Anesthesia and surgical procedures

Sixteen beagles was obtained from the Laboratory Animal Center of the Southern Medical University with a mean body weight about 10 kg. Briefly, general anesthesia was induced by midazolam (10mg, intravenous), followed by the procedure of tracheotomy with an endotracheal tube properly inserted. We established the venous line via the left internal jugular vein. Intra-operative anesthesia was maintained by the intravenous administration of fentanyl (150 μg/kg) and the inhalation of 2.5% sevoflurane through the endotracheal tube, which was then connected to a mechanical ventilator for experimental animals (HX-300S, Taimeng Inc., Chengdu, China). The ventilator supported at a rate of 22 times/minute, and the tidal volume was set at 10mL/kg/respiration. The right common carotid artery and the right jugular vein were dissected, unfractionated heparin bolus (100 U/kg) was then administered intravenously, with an activated clotting time (ACT) ranging from 180 to 240 seconds. The right common carotid artery and the right jugular vein were successfully cannulated with the 8-Fr and 10-Fr cannulas (Medtronic Inc., Minneapolis, MN, USA), respectively. A venous-arterial (V-A) ECMO was initiated at a flow rate of 130 mL/kg/min for both perfusion modes.

Animal models and monitoring

ECMO was initiated under normal cardiac condition for the first 20 minutes. Animal models of cardiogenic shock was made through ventricular fibrillation, which was created by the 4-V alternating current externally. Once the cardiogenic shock model was made, hemodynamic variables including heart rate, arterial pressure, oxygen saturation, blood gases, blood samplings, ACT, and urinary output were monitored (Truwave and Vigilance II, Edwards Lifesciences, LLC, USA). Hemodynamic data and blood samplings were collected at 6 time points: baseline, before ECMO, 15 minutes after ECMO, 1 hour after ECMO, 3 hours after ECMO, and 6 hours after ECMO. After 6 hours of ECLS, the circuit was discontinued. Phenylephrine shots were used during ECLS in case of hypotension systolic, which was defined as pressure below 30 mmHg. At the end of the experiment, animals were euthanized by potassium chloride (3 mEq/kg) under general anesthesia. The experimental ECMO circuit was shown in Fig. 1.

Pulsatility assessment

Shepard`s model was used to quantify pulsatility as described previously[12], and the following parameters were assessed:

Energy-equivalent pressure (EEP)= ∫QPdt/∫Qdt, in which Q is the blood flow (mL/s), P is the instantaneous pressure (mmHg), and t is the time (s); Surplus hemodynamic energy (SHE) = 1,332 (EEP − MAP) (ergs/cm^3), in which MAP is the mean arterial pressure[12].

Shear stress assessment

To assess wall shear stress during pulsatile ECMO, blood flow velocity (v), radius of the femoral arteries (R), and viscocity of the whole blood (η) were measured initially. The radius and velocity of the vessels were accrued using an ultrasound machine for animals (P6-VET, Dawei, Jiangsu, China). The M-mode was utilized for determining radius of the femoral artery, of which the inner radius in the end-diastolic phase was detected. Mean value of the velocities in three successional cardiac cycles was recorded. The velocity and radius of the femoral arteries were examined at the aforementioned six time points. Viscosity of the whole blood (η) was deternined at each time point by a hemorheology meter (LG-R-80E, Steellex Inc., Beijing, China).

To more precisely quantify pulsatile flow, the Womersley principle, which defined the flow by pulsatile pressure gradient, was applied[20]. The peak wall shear stress (PWSS) was used and was calculated as follows:

In this equation, η is the viscosity of the whole blood, *R* is the radius, *n* is the harmonics, *N* is the maxium of harmonics, is the n-th harmonic component of the axial blood velocity, =, and are the Bessel function of order 0 and 1, is the Womersley value, is the density, 2n is the circular frequency, and is the fundamental frequency.

Measurements of serum syndecan-1 and heparan sulfate

Blood samples were taken at six time points according to the experiment protocol. Serum concentrations of syndecan-1 and heparan sulfate were detected using the enzyme-linked immunosorbent assay (ELISA)

kits (Renjiebio Co., Shanghai, China).

PMVECs isolation and culture

20 male SD rats ranging from 100 to 150g were obtained from the Laboratory Animal Center of the Southern Medical University. The rats were sacrificed after general anesthesia by intraperitoneal administration of pentobarbital (30mg/kg). Lung tissues were separated and collected in the absence of pleura and large vessels. Tissues were then cut into slices and were kept in culture flasks. Tissues were cultivated at 5% CO2 in room temperature for 4 days, with 15% fetal bovine serum added. PMVECs were then isolated, and we changed the mediums every two days. Rat PMVECs were cultured in line with the proven techniques in our laboratory, as described previously[21].

In vitro flow shear stress experiments

Pulstile shear stress experiments were conducted in vitro using the Flexcell apparatus (Flexcell™ Inc., McKee-sport, PA, USA), which applied fluid shear stresses to PMVECs under various conditions. PMVECs were seeded on a 6-well Flexcell plates and incubated for 2 days. Seeded PMVECs (1×10^5 cells per well) were deprived from FBS and exposed to continuous flow or pulsatile flow, with frequency set at 1 Hz. Different degrees of pulsatility were applied, low pulsatility, intermittent pulsatility, and the high pulsatility, which were defined as pulsatile flow at 5 dyne/cm^2, 10 dyne/cm^2, and 20 dyne/cm^2, respectively. The flow rate was maintained at about 2mL/min. PMVECs were cultured and treated with various shear stress settings for 6 hours.

Cell viability assay

At the end of the flow experiment, PMVECs viability was assessed using the CCK-8 kits. PMVECs were placed in the 96-well plate under humidified environment (5% CO_2/95% air) at 37℃ overnight. 10μL CCK-8 was added to the wells, where PMVECs were additionally incubated 3 hours at 37℃. The absorbance at 450 nm reflected cell viability and was detected using the Microplate Reader (Enspire, PerkinElmer, MA, USA).

RNA isolation and quantitative RT-PCR

PMVECs were lysed with the Trizol reagent (ThermoFisher Scientific, MA, USA), and total RNAs were extracted with the RNeasy Mini Kit (Qiagen, Cary, NC, USA) after the completion of shear stress experiments. The extracted RNAs were reversed transcribed using the Oligo (dT) primers and samples were prepared by mixing complementary DNA, specific primers, and power-SYBR Mix (Yeason Biotech Co., Shanghai, China). Quantitative RT-PCR was performed using the LightCycler 480 (Roche, Basel, Swizerland) according to the manufacturer`s instructions. Each experiment was performed thrice. Expressions of syndecan-1 mRNA, EndMT markers (ACTA2, Snail1), and PECAM-1 were measured. Expression levels of each mRNAs were measured with the comparative cycle threshold (ΔΔCT) approach. Level of the non-pulsatile condition was set to be 1. Expressions of genes were normalized to GADPH as a housekeeping gene. Primers used in the present study were listed in Table 1.

Table 1
Primers for qRT-PCR.

Genes	Primer sequences
Syndecan-1	Forward 5'-TCTGACAACTTCTCCGGCTC-3'
	Reverse 5'-CCACTTCTGGCAGGACTACA-3'
ACTA2	Forward 5'-TCCATCCTGGCCTCTCTGT-3'
	Reverse 5'-GCTTCGTCGTACTCCTGTT-3'
Snail1	Forward 5'-GCCCAACTACAGCGAGCTAC-3'
	Reverse 5'-CCAGGAGAGACTCCCAGATG-3'
PECAM-1	Forward 5'-ATCTGCATCTCGTGGGAAGT-3'
	Reverse 5'-GAGCTGAAGTGTCAGCAGGA-3'
GADPH	Forward 5'-GGGTGTGAACCACGAGAAAT-3'
	Reverse 5'-ACTGTGGTCATGAGCCCTTC-3'

Statistics

Statistical analyses were conducted with IBM SPSS Statistics version 16.0 software (SPSS Inc., Chicago, IL, USA). Continuous variables were displayed as mean ± standard deviation (SD). Wilcoxon signed-rank test was used to compare differences at different time points, and the Spearman rank correlation coefficient was applied for the analysis of correlation. Comparisons for multiple time points and different flow settings were performed using the repeated measures of analysis of variance (ANOVA). All hypotheses in the present study were two-sided and all p values below 0.05 were considered to be statistically significant.

Results

Pulsatility assessment

All circuits ran uneventfully for 6 hours, without major adverse effects. Figure 2 displays the waveforms of femoral arteries during ECLS in non-pulsatile or pulsatile fashion, in which the diastolic enhancement was seen. As shown in Table 2, the hematocrit, hemoglobin, and platelet counts decreased over time, while leukocyte counts and the level of lactic acid increased during ECLS, however, no between-group differences were noted. After the initiation of ECMO, MAP decreased in both groups, while MAP levels were significantly higher in the pulsatile group at between 3 hours and 6 hours (Table 3). Similarly, higher levels of EEP were observed in the pulsatile group at between 1 hour and 6 hours during ECMO, at all time points. Accordingly, the pulsatile flow generated more SHE than did the non-pulsatile flow at between 1 hour and 6 hours, at all time points, based on Shepard’s model (Table 3).

Table 2
Blood parameters of the ECMO circuits.

	Baseline	Before ECMO	ECMO 15 min	ECMO 1 hour	ECMO 3 hours	ECMO 6 hours
Hematocrit (%)						
Non-pulsatile group (n = 8)	33.0 ± 12.3	30.9 ± 14.7	28.5 ± 19.1	24.6 ± 9.5	23.8 ± 10.0	22.7 ± 9.8
Pulsatile group (n = 8)	29.6 ± 14.6	29.2 ± 10.8	29.0 ± 9.0	26.2 ± 10.2	22.5 ± 11.4	20.4 ± 12.9
Lactic Acid (mmol/L)						
Non-pulsatile group (n = 8)	0.7 ± 0.3	1.5 ± 0.9	1.2 ± 0.8	2.5 ± 1.3	3.7 ± 1.4	2.8 ± 1.6
Pulsatile group (n = 8)	1.1 ± 0.7	1.5 ± 0.6	1.7 ± 1.3	2.1 ± 1.2	2.7 ± 1.9	3.1 ± 1.8
Hemoglobin (g/L)						
Non-pulsatile group (n = 8)	99.2 ± 34.4	98.6 ± 29.1	82.7 ± 36.6	77.9 ± 28.1	73.5 ± 37.0	68.6 ± 31.9
Pulsatile group (n = 8)	93.5 ± 49.0	90.5 ± 46.5	80.8 ± 49.3	75.1 ± 32.2	69.4 ± 24.2	63.4 ± 47.7
White blood cell count (×10^9/L)						
Non-pulsatile group (n = 8)	8.9 ± 3.8	9.1 ± 4.0	10.8 ± 5.0	12.1 ± 5.8	13.6 ± 6.6	14.1 ± 7.9
Pulsatile group (n = 8)	9.2 ± 4.1	9.7 ± 3.3	10.5 ± 4.9	11.7 ± 4.4	13.0 ± 5.5	13.3 ± 6.7
Platelet count (×10^9/L)						
Non-pulsatile group (n = 8)	150.1 ± 63.4	140.6 ± 68.7	130.7 ± 69.9	126.5 ± 50.0	133.1 ± 57.8	107.4 ± 49.6
Pulsatile group (n = 8)	161.4 ± 59.8	157.6 ± 74.1	131.8 ± 52.5	134.8 ± 73.6	121.9 ± 60.3	110.6 ± 65.2

Table 3
Pulsatility parameters of the ECLS circuits.

	Baseline	Before ECMO	ECMO 15 min	ECMO 1 hour	ECMO 3 hours	ECMO 6 hours
MAP (mmHg)						
Non-pulsatile group	59.5 ± 16.4	67.3 ± 21.1	48.8 ± 9.7	35.4 ± 7.5	33.8 ± 6.9	32.2 ± 6.3
Pulsatile group	60.6 ± 11.7	65.2 ± 17.3	52.1 ± 21.0	42.1 ± 13.6	43.4 ± 9.1*	41.9 ± 10.0*
CVP (mmHg)						
Non-pulsatile group	3.7 ± 1.3	4.3 ± 0.9	4.2 ± 0.6	4.5 ± 2.0	3.9 ± 0.4	4.3 ± 1.5
Pulsatile group	3.1 ± 0.8	3.9 ± 1.6	4.0 ± 2.1	4.1 ± 1.2	4.2 ± 1.4	4.5 ± 0.8
EEP (mmHg)						
Non-pulsatile group	59.3 ± 13.2	68.1 ± 12.4	42.5 ± 15.3	36.1 ± 18.0	38.5 ± 8.4	33.6 ± 6.5
Pulsatile group	53.4 ± 9.1	63.5 ± 25.8	49.9 ± 8.6	46.8 ± 7.7*	47.6 ± 11.3*	44.4 ± 5.3#
SHE (erg/cm^3)						
Non-pulsatile group	2125.5 ± 965.4	2011.1 ± 864.3	2317.8 ± 640.4	455.7 ± 98.4	661.3 ± 98.5	698.7 ± 98.6
Pulsatile group	1913.2 ± 687.0	1845.3 ± 657.5	1987.5 ± 543.1	1718.6 ± 431.9#	1905.5 ± 673.8#	1795.5 ± 612.2#

Shear stress evaluation

Based on Womersley`s theory, Fig. 3A shows the PWSS values of the femoral artery during ECLS. After the commencement of ECMO, the PWSS values decreased gradually in both groups, nonetheless, the pulsatile group had higher PWSS levels than did the non-pulsatile group from 15 min to 6 hours during ECLS. PWSS nadirs occurred at 6 hours during ECLS in both groups, reaching averages of 3.125 ± 0.83 and 14.88 ± 3.18 dyne/cm^2, respectively. The PWSS values were positively correlated with EEP ($r = 0.70$, $p < 0.01$) and SHE ($r = 0.73$, $p < 0.01$), as shown in Fig. 3B and 3C.

Serum concentrations of syndecan-1 and heparan sulfate

The baseline serum levels of syndecan-1 in the pulsatile group and non-pulsatile group achieved average values of 1.69 ± 0.80 and 1.68 ± 0.79 μg/dL, respectively. The serum syndecan-1 concentration increased after the commencement of ECMO, and reached its summit at 6 hours during ECMO (Fig. 4A). The values at 6 hours were approximately 6.5 and 13.3 times of the baseline levels in these two group, respectively.

The syndecan-1 levels in the pulsatile group at 6 hours were significantly lower as compared with the non-pulsatile group ($p < 0.01$). Similarly, the serum levels of heparan sulfate also increased after ECLS and peaked at 6 hours, equivalent to 1.4 and 5.1 times ot the baseline levels in the pulsatile group and non-pulsatile group, respectively, and again, the pulsatile group had lower heparan sulfate levels than did the non-pulsatile group ($p < 0.05$), as shown in Fig. 4B.

Correlations of PWSS with syndecan-1 and heparan sulfate

The PWSS levels during ECLS were negatively correlated with serum syndecan-1 concentrations ($r=-0.61$, $p < 0.01$) and heparan sulfate ($r=-0.57$, $p < 0.01$)(Fig. 4C and 4D), suggesting that PWSS during ECLS maintains the integrity of endothelial glycocalyx.

Responses of endothelial cells to pulsatility

We investigated the cell viability responses of PMVECs following incubations of non-pulsatile or pulsatile flows (low, intermittent, or high pulsatility), and we found no difference in cell viability among these cultural conditions using the CCK-8 assay (Fig. 5A). We further investigated the endothelial glycocalyx related gene expressions under these cultural conditions. Using static condition as the reference, exposure to non-pulsatile flow significantly up-regulated the mRNA expression of syndecan-1 in PMVECs as compared to pulsatile flows ($p < 0.01$). In additonal, PMVECs that exposed to low pulsatility (5 dyne/cm^2) had lower syndecan-1 expressions as compared to high pulsatility (20 dyne/cm^2)($p < 0.05$), as shown in Fig. 5B.

Moreover, we studied the possibility of phenotypic alteration of EndMT in PMVECs under various pulsatile conditions (Fig. 5C-D). Compared to pulsatile conditions, the non-pulsatile flow significantly upregulated EndMT-related genes including ACTA2 and Snail-1. No differences of ACTA2 expressions were reached among low, intermittent, and high pulsatility, however, the high pulsatility group had higher expressions of Snail-1 than did the low pulsatility group (Snail-1 expression 2.1 ± 0.4 fold increase over non-pulsatility, $p < 0.01$) and the intermittent pulsatility group (Snail-1 expression 1.7 ± 0.5 fold increase over non-pulsatility, $p < 0.05$). Finally, we analyzed the expression of PECAM-1, the indicator of endothelial phenotype (Fig. 5E). On the contrary, lower level of PECAM-1 expression was obseved in the non-pulsatile group (54 ± 11% of the static control), as compared to low pulsatile or intermittent conditions. Higher expression of PECAM-1 was seen in PMVEC exposed to low pulsatility (84 ± 5% of the static control), as compared to the high pulsatility (64 ± 15% of the static control, $p < 0.05$).

Discussion

The hemodynamic advantages of pulsatile flow have been generally acknowledged in the mechanical circulatory support systems, however, whether pulsatile flow improves microcirculation and preserves endothelial integrity has to be confirmed. In the present study, we found that the pulsatile flow generates more SHE and maintains higher PWSS during ECMO as compared to the non-pulsatile flow. The levels of syndecan-1 and heparan sulfate, which are negatively correlated with PWSS, were significantly higher in the non-pulsatile group, indicating that PWSS during ECMO has beneficial effects on endothelial integrity.

Moreover, our findings show that non-pulsatility facilitates EndMT, upregulating EndMT related genes, whereas low pulsatility exerts the best protective effects.

ECMO is a life-saving device that rescues the cardiorespiratory sytem, however, the conventional non-pulsatile flow during prolonged ECLS may result in microcirculatory disturbance, which is detrimental to the outcome for ECMO[4]. It has been confirmed that the alteration of flow pattern during ECLS declines flow velocities and PWSS[19]. The endothelial glycocalyx, a mechanosensor, receives the signals of hemodynamic and shear stress changes, affecting the synthesis and biological functions of glycocalyx[22]. It has been reported that the degradation of glycocalyx treated with non-pulsatile flow is significantly higher as compared to pulsatile flow[23]. A relatively low PWSS also promotes the glycocalyx degradation and thus impairs the microcirculatory integrity[24, 25]. Wang's group[26] recently reported that wall shear stress is closely relevant to glycocalyx shedding during cardiopulmonary bypass, and the non-pulsatile flow contributes to the decomposition of glycocalyx. In this study, we found that the PWSS during ECMO is positively correlated with SHE, the extra energy produced by pulsatile flow, whereas negative correlations were also observed in PWSS with glycocalyx biomarkers, suggesting that the pulsatile flow inhibits the endothelial glycocalyx degradation as it maintains some PWSS during ECMO.

Syndecan-1 and heparan sulfate are components on the surface of the glycocalyx network, and were frequently applied to indicate the glycocalyx integrity. When mast cells are activated by inflammation, ischemia, or hypoxia, matrix metalloprotease is upregulated [27], resulting in the cleavage of syndecan-1[28]. Chou et al.[29] found that the expression of matrix metalloprotease genes can be also upregulated due to the alteration of flow-related shear stress. We found that not only serum levels of syndecan-1, but also mRNA expressions in cellular level were significantly higher under non-pulsatile flow as compared to the pulsatile flow. Besides shear stress changes, the increase of syndecan-1 can be induced by various conditions[16]. Our findings, however, show that the endothelial cells directly sense the changes in pulsatility, yielding the changes in the expressions of glycocalyx-related genes correspondingly. Moreover, our findings also indicate that the acute changes of pulsatility and subsequent activation of inflammation during ECMO cause an acute release of syndecan-1 and heparan sulfate, stored in the glycocalyx network.

It is well-acknowdedged that the biological activities of endothelial cells behave differently to the magnitude of flow stress[30, 31]. Cell alignment and elongation are seen when the magnitude of flow shear stress increases[32, 33]. Faure et al.[34] reported that endothelial elongation and orientation were observed with the increase of pulsatile wall shear stress, contributing to subsequent phenotypic changes and transcriptional difference in endothelial cells. Hellmann et al.[35] also found that the endothelial cell morphology, integrity, and expressions of typical endothelial markers could be remained in pulsatile shear stress up to 8.6 dyne/cm^2. In the present study, we observed that PMVECs exposed to low pulsatility preserves glycocalyx integrity and had lower phenotypic transformation, as the syndecan-1 and EndMT related genes expressions were significantly in PMVECs exposed to high pulsatility. These results agree well with our previously study that used pulsatile flow during cardiopulmonary bypass in pediatric

patients undergoing congenital cardiac surgeries, and the results showing that low pulsatility has better hemodynamic profiles, organ protective effects, and better oxidative status[12].

EndMT is an endothelial phenotypic alteration relevant to various cardiovascular diseases and mechanical microenvironment. The pathological process of EndMT starts when the cell-cell interactions of the endothelial cells are deprived, with a series of subsequent changes in biological behaviors, such as the separation from the monolayer, migration into the interstitial space, and the lost of endothelial markers[36]. This change in phenotype as well as the transcriptional difference occurs in endothelial cells in their response to biofluid flow[37]. Several studies have shown that the development of EndMT is induced by the disturbance of shear stress and is often associated with inflammatory activation and tissue degeneration[34, 38]. In our observations, over-expressions of ACTA2 and Snail-1, the EndMT-related genes, were seen in PMVECs exposed to non-pulsatile flow, while relatively higher expression of PECAM-1 were observed in PMVECs exposed to low pulsatility, suggesting that low pulsatility has lower tendency of phenotypic transformation and protects the endothelium.

The mechanical circulatory support devices depend not only on the nature of the pump itself but also on the pattern of the flow (pulsatile or non-pulsatile) delivered by both of the pump and the left ventricle[31]. In patients with long-term mechanical circulatory support, the pulsatility is associated both with the left ventricular contractivity and the pump itself[39, 40]. In addition to hemodynamics, pulsatility in these devices seems to improve hemocompatibility, prevent bleeding complications, avoid von Willebrand Factor deficiency, and reduce systemic inflammation[31, 41].

In fact, in those critically ill COVID-19 patients with severe respiratory failure, ECLS typically lasts for weeks or even months, thus devices that provide more effective microcirculatory perfusion is optimal. Flow modification allowing for an augmentation of pump pulsatility in ECMO is now under investigation. In addtion to the i-Cor system, other recent reported pulsatile flow generators included the Medos Deltastream DP3 system (Medos Medizintechnik AG, USA)[42] and the K-Beat system by Inamori's group[8]. Overall, the development of the future ECMO devices will require an aviailability of pulsatility to reduce the complication of microcirculatory malperfusion.

Conclusion

The pulsatile flow produces more SHE and preserves more effective PWSS during ECMO. The levels of syndecan-1 and heparan sulfate are negatively correlated with PWSS, and are significantly lower under the pulsatile ECLS circuit, indicating that the pulsatility during ECMO protects the glycocalyx and the endothelial integrity. Moreover, pulsatility prevents EndMT of the endothelial cells, and low pulsatility has the best protective effects. Our data indicate that the modification of pulsatility may be a therapeutic strategy to improve the outcome in ECMO.

Declarations

Acknowledgements: None

Authors' contributions: GHL designed and supervised the research. GHL and JFZ designed the experiments. YZ, JNL, and XQH performed the experiments. JNL and XQH analyzed the data. YZ and GHL wrote the manuscript. Each author had reviewed and approved the final version of the manuscript.

Funding: This study was supported by a grant from the Traditional Chinese Medicine Bureau of Guangdong Province (No.20212071).

Availability of data and materials: The data used for this study are available from the corresponding author upon reasonable request.

Ethics approval and consent to participate: Ethical approval was obtained from the Institutional Animal Care and Use Committee of Sun Yat-sen Memorial Hospital (Reference No. SYSU-IACUC-2020-B0402).

Consent for publication: Not applicable.

Competing Interests: All authors declare no competing interests.

References

[1] R.P. Barbaro, G. MacLaren, P.S. Boonstra, T.J. Iwashyna, A.S. Slutsky, E. Fan, R.H. Bartlett, J.E. Tonna, R. Hyslop, J.J. Fanning, P.T. Rycus, S.J. Hyer, M.M. Anders, C.L. Agerstrand, K. Hryniewicz, R. Diaz, R. Lorusso, A. Combes, D. Brodie, Extracorporeal membrane oxygenation support in COVID-19: an international cohort study of the Extracorporeal Life Support Organization registry, Lancet (London, England) 396(10257) (2020) 1071-1078.

[2] M. Matteucci, D. Fina, F. Jiritano, P. Meani, G.M. Raffa, M. Kowalewski, I. Aldobayyan, M. Turkistani, C. Beghi, R. Lorusso, The use of extracorporeal membrane oxygenation in the setting of postinfarction mechanical complications: outcome analysis of the Extracorporeal Life Support Organization Registry, Interactive cardiovascular and thoracic surgery 31(3) (2020) 369-374.

[3] P. Adedayo, S. Wang, A.R. Kunselman, A. Ündar, Impact of Pulsatile Flow Settings on Hemodynamic Energy Levels Using the Novel Diagonal Medos DP3 Pump in a Simulated Pediatric Extracorporeal Life Support System, World journal for pediatric & congenital heart surgery 5(3) (2014) 440-8.

[4] C. Scorcella, E. Damiani, R. Domizi, S. Pierantozzi, S. Tondi, A. Carsetti, S. Ciucani, V. Monaldi, M. Rogani, B. Marini, E. Adrario, R. Romano, C. Ince, E.C. Boerma, A. Donati, MicroDAIMON study: Microcirculatory DAlly MONitoring in critically ill patients: a prospective observational study, Annals of intensive care 8(1) (2018) 64.

[5] F. Born, F. König, J. Chen, S. Günther, C. Hagl, N. Thierfelder, Generation of microbubbles in extracorporeal life support and assessment of new elimination strategies, Artificial organs 44(3) (2020) 268-277.

[6] A. Chong, Z. Sun, L. van de Velde, S. Jansen, M. Versluis, M. Reijnen, E. Groot Jebbink, A novel roller pump for physiological flow, Artificial organs 44(8) (2020) 818-826.

[7] S. Wang, J.M. Izer, J.B. Clark, S. Patel, L. Pauliks, A.R. Kunselman, D. Leach, T.K. Cooper, R.P. Wilson, A. Ündar, In Vivo Hemodynamic Performance Evaluation of Novel Electrocardiogram-Synchronized Pulsatile and Nonpulsatile Extracorporeal Life Support Systems in an Adult Swine Model, Artif Organs 39(7) (2015) E90-e101.

[8] Y. Fujii, N. Akamatsu, Y. Yamasaki, K. Miki, M. Banno, K. Minami, S. Inamori, Development of a Pulsatile Flow-Generating Circulatory Assist Device (K-Beat) For Use with Veno-Arterial Extracorporeal Membrane Oxygenation in a Pig Model Study, Biology 9(6) (2020).

[9] T. Fleck, C. Benk, R. Klemm, J. Kroll, M. Siepe, J. Grohmann, R. Höhn, F. Humburger, F. Beyersdorf, B. Stiller, First serial in vivo results of mechanical circulatory support in children with a new diagonal pump, European journal of cardio-thoracic surgery : official journal of the European Association for Cardio-thoracic Surgery 44(5) (2013) 828-35.

[10] P. Ostadal, M. Mlcek, H. Gorhan, I. Simundic, S. Strunina, M. Hrachovina, A. Krüger, D. Vondrakova, M. Janotka, P. Hala, M. Mates, M. Ostadal, J.C. Leiter, O. Kittnar, P. Neuzil, Electrocardiogram-synchronized pulsatile extracorporeal life support preserves left ventricular function and coronary flow in a porcine model of cardiogenic shock, PloS one 13(4) (2018) e0196321.

[11] E. Kadiroğulları, O. Sen, S. Gode, S. Basgoze, B. Timur, A. Basgoze, Ü. Aydin, B. Onan, Effect of Pulsatile Cardiopulmonary Bypass in Adult Heart Surgery, The heart surgery forum 23(3) (2020) E258-e263.

[12] G. Li, W. Jiang, Y. Zhang, X. Zhang, J. Chen, J. Zhuang, C. Zhou, The outcome of pediatric patients undergoing congenital cardiac surgery under pulsatile cardiopulmonary bypass in different frequencies, Ther Clin Risk Manag 14 (2018) 1553-1561.

[13] A. Salameh, L. Kühne, M. Grassl, M. Gerdom, S. von Salisch, M. Vollroth, F. Bakhtiary, F.W. Mohr, I. Dähnert, S. Dhein, Protective effects of pulsatile flow during cardiopulmonary bypass, The Annals of thoracic surgery 99(1) (2015) 192-9.

[14] H. Okada, S. Yoshida, A. Hara, S. Ogura, H. Tomita, Vascular endothelial injury exacerbates coronavirus disease 2019: The role of endothelial glycocalyx protection, Microcirculation (New York, N.Y. : 1994) (2020) e12654.

[15] C. Chelazzi, G. Villa, P. Mancinelli, A.R. De Gaudio, C. Adembri, Glycocalyx and sepsis-induced alterations in vascular permeability, Critical care (London, England) 19(1) (2015) 26.

[16] M. Rehm, D. Bruegger, F. Christ, P. Conzen, M. Thiel, M. Jacob, D. Chappell, M. Stoeckelhuber, U. Welsch, B. Reichart, K. Peter, B.F. Becker, Shedding of the endothelial glycocalyx in patients undergoing

major vascular surgery with global and regional ischemia, Circulation 116(17) (2007) 1896-906.

[17] H. Yang, L. Zhu, Y. Chao, Y. Gu, X. Kong, M. Chen, P. Ye, J. Luo, S. Chen, Hyaluronidase2 (Hyal2) modulates low shear stress-induced glycocalyx impairment via the LKB1/AMPK/NADPH oxidase-dependent pathway, Journal of cellular physiology 233(12) (2018) 9701-9715.

[18] N.A.M. Dekker, D. Veerhoek, N.J. Koning, A.L.I. van Leeuwen, P.W.G. Elbers, C.E. van den Brom, A.B.A. Vonk, C. Boer, Postoperative microcirculatory perfusion and endothelial glycocalyx shedding following cardiac surgery with cardiopulmonary bypass, Anaesthesia 74(5) (2019) 609-618.

[19] A. Assmann, A.C. Benim, F. Gül, P. Lux, P. Akhyari, U. Boeken, F. Joos, P. Feindt, A. Lichtenberg, Pulsatile extracorporeal circulation during on-pump cardiac surgery enhances aortic wall shear stress, Journal of biomechanics 45(1) (2012) 156-63.

[20] C.A. Leguy, E.M. Bosboom, A.P. Hoeks, F.N. van de Vosse, Model-based assessment of dynamic arterial blood volume flow from ultrasound measurements, Medical & biological engineering & computing 47(6) (2009) 641-8.

[21] G. Li, Z. Hu, H. Yin, Y. Zhang, X. Huang, S. Wang, W. Li, A novel dendritic nanocarrier of polyamidoamine-polyethylene glycol-cyclic RGD for "smart" small interfering RNA delivery and in vitro antitumor effects by human ether-à-go-go-related gene silencing in anaplastic thyroid carcinoma cells, International journal of nanomedicine 8 (2013) 1293-306.

[22] F. Sangalli, M. Guazzi, S. Senni, W. Sala, R. Caruso, M.C. Costa, F. Formica, L. Avalli, R. Fumagalli, Assessing Endothelial Responsiveness After Cardiopulmonary Bypass: Insights on Different Perfusion Modalities, Journal of cardiothoracic and vascular anesthesia 29(4) (2015) 912-6.

[23] R. Uchimido, E.P. Schmidt, N.I. Shapiro, The glycocalyx: a novel diagnostic and therapeutic target in sepsis, Critical care (London, England) 23(1) (2019) 16.

[24] S. Elhadj, S.A. Mousa, K. Forsten-Williams, Chronic pulsatile shear stress impacts synthesis of proteoglycans by endothelial cells: effect on platelet aggregation and coagulation, Journal of cellular biochemistry 86(2) (2002) 239-50.

[25] B.F. Becker, M. Jacob, S. Leipert, A.H. Salmon, D. Chappell, Degradation of the endothelial glycocalyx in clinical settings: searching for the sheddases, British journal of clinical pharmacology 80(3) (2015) 389-402.

[26] G. He, Y. Gao, L. Feng, G. He, Q. Wu, W. Gao, L. Lin, W. Wang, Correlation Between Wall Shear Stress and Acute Degradation of the Endothelial Glycocalyx During Cardiopulmonary Bypass, Journal of cardiovascular translational research 13(6) (2020) 1024-1032.

[27] S. Pasta, V. Agnese, A. Gallo, F. Cosentino, M. Di Giuseppe, G. Gentile, G.M. Raffa, J.F. Maalouf, H.I. Michelena, D. Bellavia, P.G. Conaldi, M. Pilato, Shear Stress and Aortic Strain Associations With

Biomarkers of Ascending Thoracic Aortic Aneurysm, The Annals of thoracic surgery 110(5) (2020) 1595-1604.

[28] M.M. Ali, A.M. Mahmoud, E. Le Master, I. Levitan, S.A. Phillips, Role of matrix metalloproteinases and histone deacetylase in oxidative stress-induced degradation of the endothelial glycocalyx, American journal of physiology. Heart and circulatory physiology 316(3) (2019) H647-h663.

[29] P.H. Chou, S.T. Wang, M.H. Yen, C.L. Liu, M.C. Chang, O.K. Lee, Fluid-induced, shear stress-regulated extracellular matrix and matrix metalloproteinase genes expression on human annulus fibrosus cells, Stem cell research & therapy 7 (2016) 34.

[30] A.A. Polk, T.M. Maul, D.T. McKeel, T.A. Snyder, C.A. Lehocky, B. Pitt, D.B. Stolz, W.J. Federspiel, W.R. Wagner, A biohybrid artificial lung prototype with active mixing of endothelialized microporous hollow fibers, Biotechnology and bioengineering 106(3) (2010) 490-500.

[31] F. Vincent, A. Rauch, V. Loobuyck, E. Robin, C. Nix, A. Vincentelli, D.M. Smadja, P. Leprince, J. Amour, G. Lemesle, H. Spillemaeker, N. Debry, C. Latremouille, P. Jansen, A. Capel, M. Moussa, N. Rousse, G. Schurtz, C. Delhaye, C. Paris, E. Jeanpierre, A. Dupont, D. Corseaux, M. Rosa, Y. Sottejeau, S. Barth, C. Mourran, V. Gomane, A. Coisne, M. Richardson, C. Caron, C. Preda, A. Ung, A. Carpentier, T. Hubert, C. Denis, B. Staels, P.J. Lenting, E. Van Belle, S. Susen, Arterial Pulsatility and Circulating von Willebrand Factor in Patients on Mechanical Circulatory Support, Journal of the American College of Cardiology 71(19) (2018) 2106-2118.

[32] X. Zhang, D.J. Huk, Q. Wang, J. Lincoln, Y. Zhao, A microfluidic shear device that accommodates parallel high and low stress zones within the same culturing chamber, Biomicrofluidics 8(5) (2014) 054106.

[33] E. Min, M.A. Schwartz, Translocating transcription factors in fluid shear stress-mediated vascular remodeling and disease, Experimental cell research 376(1) (2019) 92-97.

[34] E. Faure, E. Bertrand, A. Gasté, E. Plaindoux, V. Deplano, S. Zaffran, Side-dependent effect in the response of valve endothelial cells to bidirectional shear stress, International journal of cardiology 323 (2021) 220-228.

[35] A. Hellmann, S. Klein, F. Hesselmann, S. Djeljadini, T. Schmitz-Rode, S. Jockenhoevel, C.G. Cornelissen, A.L. Thiebes, EndOxy: Mid-term stability and shear stress resistance of endothelial cells on PDMS gas exchange membranes, Artificial organs (2020).

[36] G.J. Mahler, C.M. Frendl, Q. Cao, J.T. Butcher, Effects of shear stress pattern and magnitude on mesenchymal transformation and invasion of aortic valve endothelial cells, Biotechnology and bioengineering 111(11) (2014) 2326-37.

[37] J.T. Butcher, A.M. Penrod, A.J. García, R.M. Nerem, Unique morphology and focal adhesion development of valvular endothelial cells in static and fluid flow environments, Arteriosclerosis, thrombosis, and vascular biology 24(8) (2004) 1429-34.

[38] G.J. Mahler, E.J. Farrar, J.T. Butcher, Inflammatory cytokines promote mesenchymal transformation in embryonic and adult valve endothelial cells, Arteriosclerosis, thrombosis, and vascular biology 33(1) (2013) 121-30.

[39] K.G. Soucy, S.C. Koenig, G.A. Giridharan, M.A. Sobieski, M.S. Slaughter, Defining pulsatility during continuous-flow ventricular assist device support, The Journal of heart and lung transplantation : the official publication of the International Society for Heart Transplantation 32(6) (2013) 581-7.

[40] S.R. Patel, U.P. Jorde, Creating adequate pulsatility with a continuous flow left ventricular assist device: just do it!, Current opinion in cardiology 31(3) (2016) 329-36.

[41] G. Li, Z. Chen, Y. Zhang, Z. Wu, J. Zheng, Effects of left ventricular assist device on heart failure patients: A bioinformatics analysis, Artificial organs 44(6) (2020) 577-583.

[42] S. Wang, A.R. Kunselman, J.B. Clark, A. Ündar, In vitro hemodynamic evaluation of a novel pulsatile extracorporeal life support system: impact of perfusion modes and circuit components on energy loss, Artificial organs 39(1) (2015) 59-66.

Figures

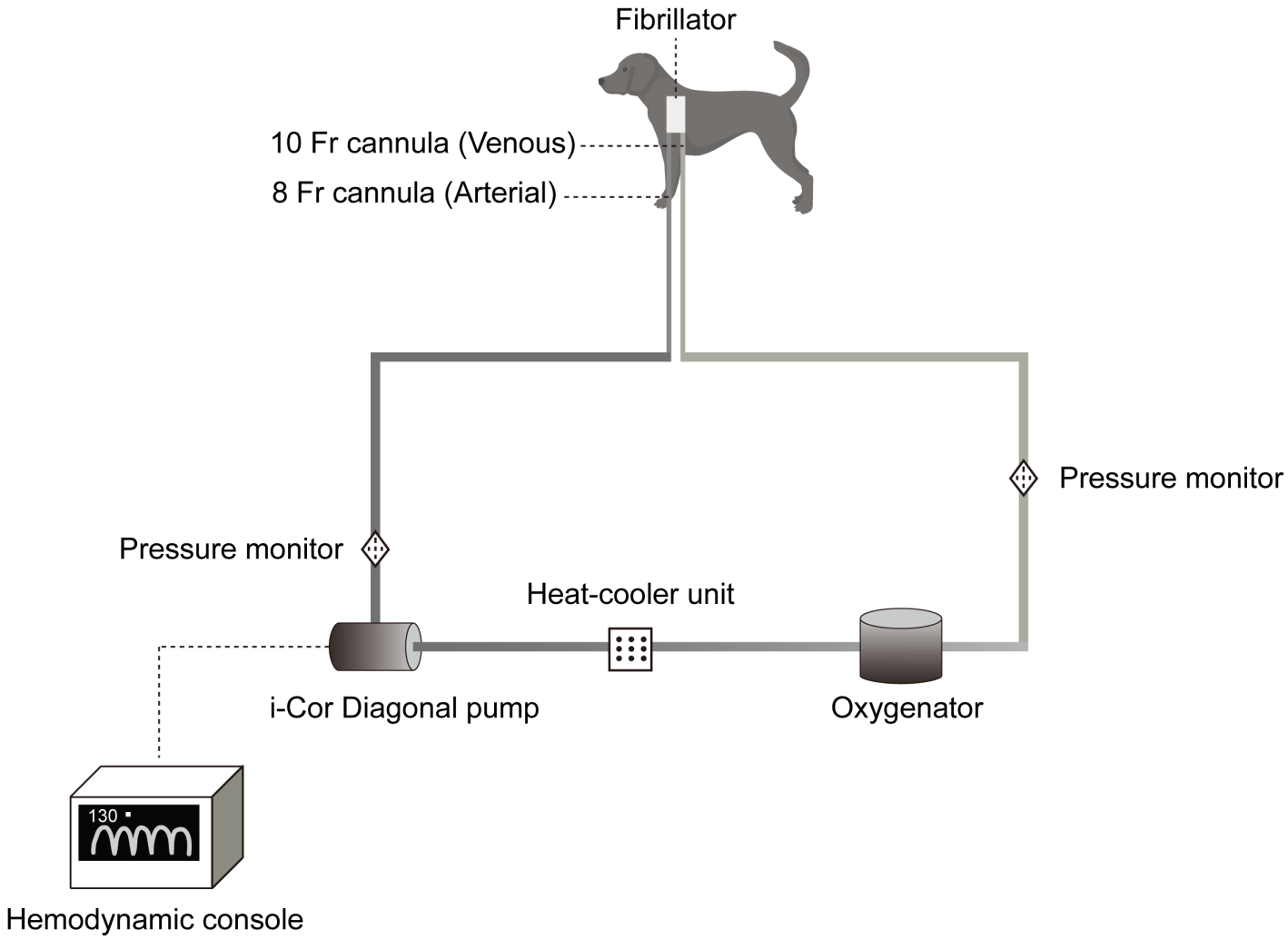

Figure 1

The experimental ECMO circuit. Abbreviations: ECMO, extracorporeal membrane oxygenation.

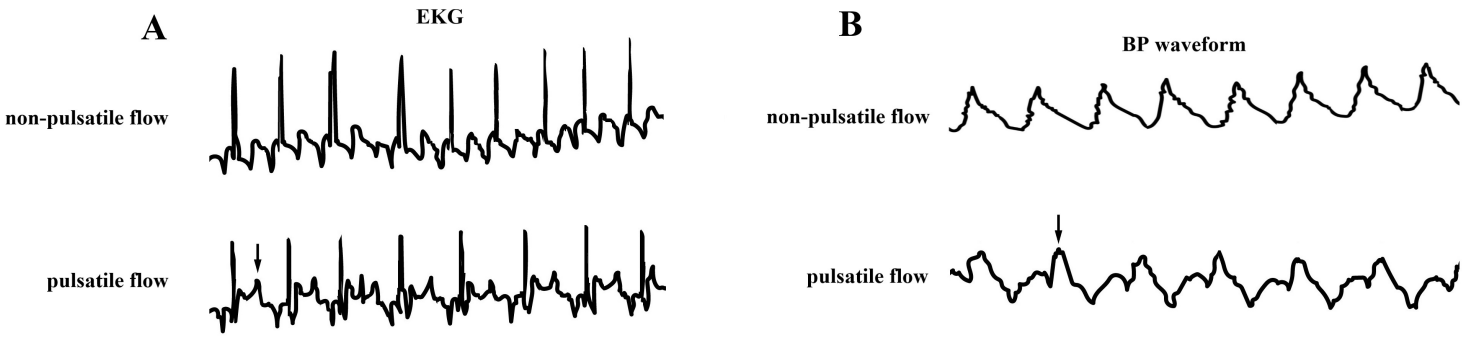

Figure 2

Electrocardiograms (Panel A) and blood pressure waveforms (Panel B) of the experimental ECMO circuits. Abbreviations: EKG, electrocardiogram; BP, blood pressure; ECMO, extracorporeal membrane

oxygenation.

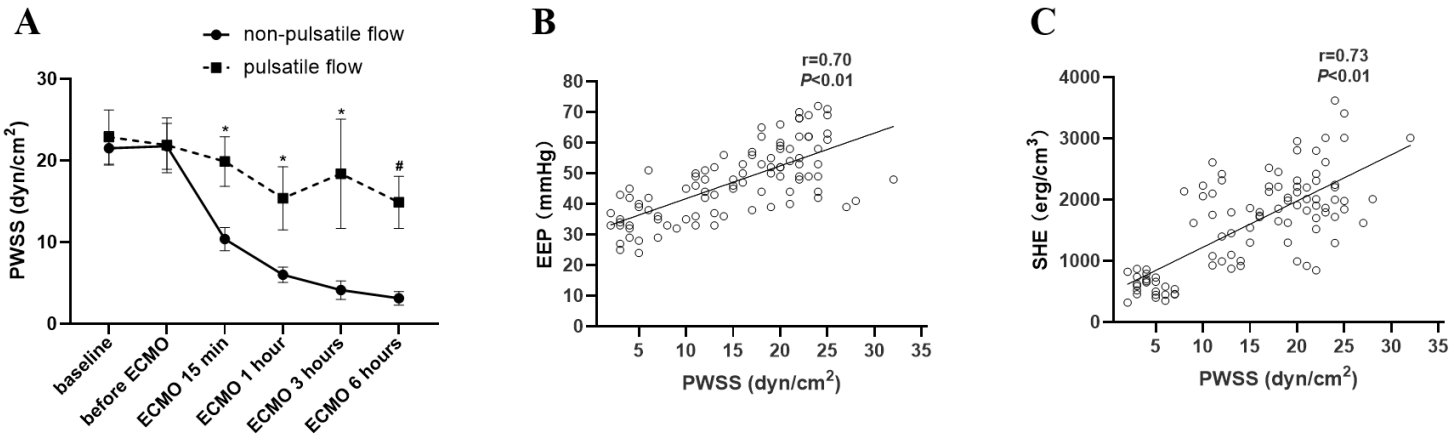

Figure 3

The changes of PWSS at different operative time-points and the correlations with hemodynamic parameters. Notes: Panel A, the changes of PWSS at different time-points during ECMO; Panel B, the correlation of PWSS with EEP; Panel C, the correlation of PWSS with SHE. *, significantly different between groups at the same time-point, p<0.05; #, significantly different between groups at the same time-point, p<0.01. Abbreviations: PWSS, peak wall shear stress; EEP, energy equivalent pressure; SHE, surplus hemodynamic energy; ECMO, extracorporeal membrane oxygenation.

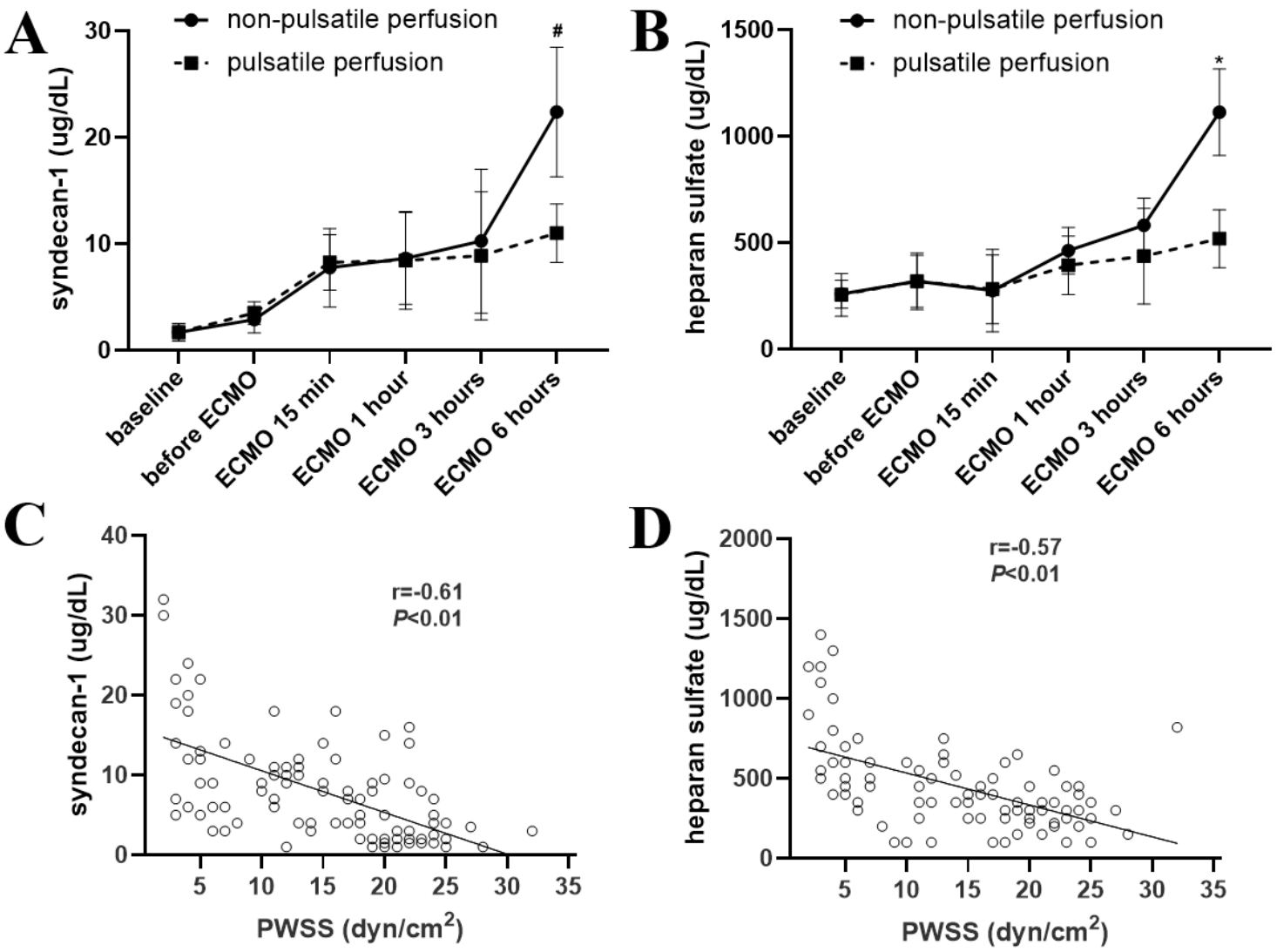

Figure 4

The changes of syndecan-1 and heparan sulfate at different operative time-points and the correlations with PWSS. Notes: Panel A, the changes of syndecan-1 levels at different time-points during ECMO; Panel B, the changes of heparan sulfate levels at different time-points during ECMO; Panel C, the correlation of syndecan-1 with PWSS; Panel D, the correlation of heparan sulfate with PWSS. *, significantly different between groups at the same time-point, $p<0.05$; #, significantly different between groups at the same time-point, $p<0.01$. Abbreviations: PWSS, peak wall shear stress; ECMO, extracorporeal membrane oxygenation.

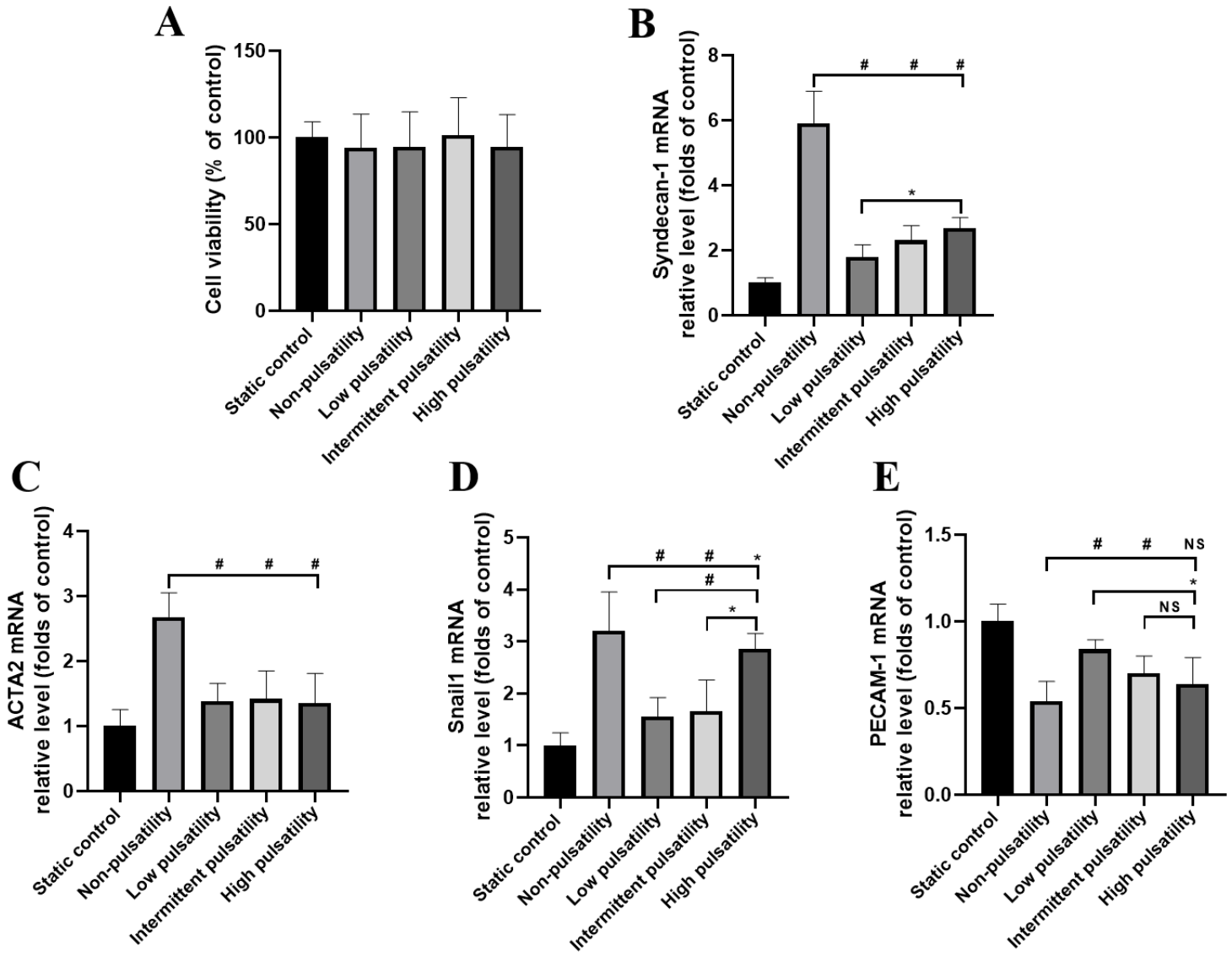

Figure 5

Responses of endothelial cells exposed to non-pulsatile flow or pulsatility at different magnitudes. Notes: Panel A, cell viabilities of endothelial cells following exposures to non-pulsatile or pulsatile flows by CCK-8 assays; Panel B, expressions of syndecan-1 mRNA by qRT-PCR; Panel C, expressions of ACTA2 mRNA by qRT-PCR; Panel D, expressions of Snail-1 mRNA by qRT-PCR; Panel E, expressions of PECAM-1 mRNA by qRT-PCR. *, significantly different between groups, $p<0.05$; #, significantly different between groups, $p<0.01$.